JACS
JOURNAL OF THE AMERICAN CHEMICAL SOCIETY

COMMUNICATION

pubs.acs.org/JACS

Oxidative Atom-Transfer to a Trimanganese Complex To Form $Mn_6(\mu^6\text{-E})$ (E = O, N) Clusters Featuring Interstitial Oxide and Nitride Functionalities

Alison R. Fout, Qinliang Zhao, Dianne J. Xiao, and Theodore A. Betley*

Department of Chemistry and Chemical Biology, Harvard University, 12 Oxford Street, Cambridge Massachusetts 02138, United States

Supporting Information

ABSTRACT: Utilizing a hexadentate ligand platform, a trinuclear manganese complex of the type $(^{H}L)Mn_3(thf)_3$ was synthesized and characterized ($[^{H}L]^{6-}$ = $[MeC(CH_2N(C_6H_4\text{-}o\text{-}NH))_3]^{6-}$). The pale-orange, formally divalent trimanganese complex rapidly reacts with O-atom transfer reagents to afford the μ^6-oxo complex $(^{H}L)_2Mn_6(\mu^6\text{-}O)(NCMe)_4$, where two trinuclear subunits bind the central O-atom and the (^{H}L) ligands cooperatively bind both trinuclear subunits. The trimanganese complex $(^{H}L)Mn_3(thf)_3$ rapidly consumes inorganic azide ($[N_3]NBu_4$) to afford a dianionic hexanuclear nitride complex $[(^{H}L)_2Mn_6(\mu^6\text{-}N)](NBu_4)_2$, which subsequently can be oxidized with elemental iodine to $(^{H}L)_2Mn_6(\mu^6\text{-}N)(NCMe)_4$. EPR and alkylation of the interstitial light atom substituent were used to distinguish the nitride from the oxo complex. The oxo and oxidized nitride complexes give rise to well-defined Mn(II) and Mn(III) sites, determined by bond valence summation, while the dianionic nitride shows a more symmetric complex, giving rise to indistinguishable ion oxidation states based on crystal structure bond metrics.

We[1] and others are investigating simple polynucleating ligands to stabilize multinuclear reaction sites to exploit the expanded redox properties[2] of the complexes or to mimic polynuclear metallocofactors.[3] Using a hexadentate amine-based platform, we have observed facile construction of polynuclear iron complexes featuring a broad range of ground-state electronic structures and redox properties which vary as a function of the ligand architecture. Use of the sterically unencumbered proton-capped ligand $(^{H}L)^{6-}$ ($[^{H}L]^{6-}$ = $[MeC(CH_2NPh\text{-}o\text{-}NH)_3]^{6-}$) gives rise to low-spin iron complexes which exhibit core-delocalized redox activity,[1a] whereas use of the bulkier silylamide ligand $(^{tbs}L)^{6-}$ ($[^{tbs}L]^{6-}$ = $[1,3,5\text{-}C_6H_9(NPh\text{-}o\text{-}NSi^tBuMe_2)_3]^{6-}$) enables stabilization of high-spin complexes capable of atom-transfer reactivity to a tri-iron core,[1b] allowing us to explore the reactivity of the trinuclear species as a molecular unit. We posited that use of the sterically less encumbered (^{H}L) ligand platform might permit oxidative atom-transfer to a trinuclear core, which in turn could afford products of higher nuclearity. Herein, we present the facile, oxidative atom-transfer chemistry to a trimanganese complex, giving rise to hexanuclear Mn_6 clusters that feature interstitial oxides and nitrides.

Reaction of $^3/_2$ equivalents of $Mn_2(N(SiMe_3)_2)_4$[4] with one equivalent of $^{H}LH_6$ in thawing tetrahydrofuran (thf) affords the complex $(^{H}L)Mn_3(thf)_3$ (**1**) in high yield (Scheme 1). Single

Scheme 1

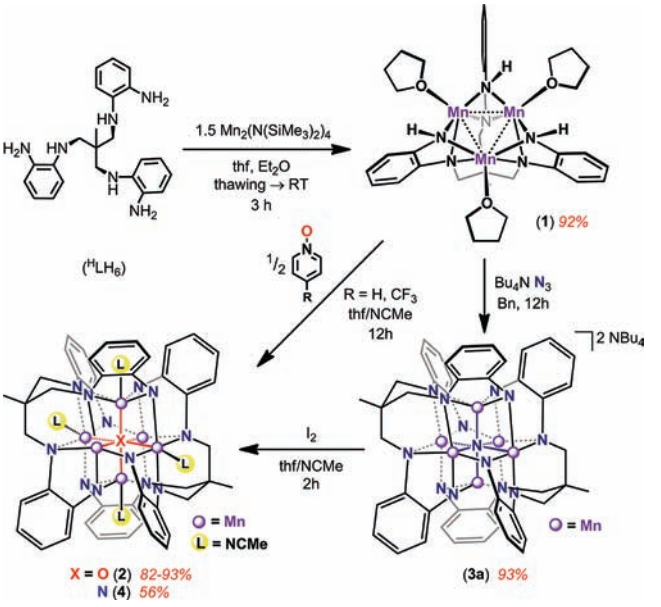

crystals of **1**, suitable for X-ray diffraction analysis, were grown from a concentrated thf solution that was allowed to stand at −35 °C. The solid-state molecular structure for **1** (see Figure S11, Supporting Information [SI]) reveals a planar arrangement of three Mn^{II} ions supported by the $[^{H}L]^{6-}$ ligand. Each Mn^{II} center resides in a square pyramidal coordination environment, with four anilide nitrogens forming the basal plane and an oxygen from a molecule of thf binding in the apical site. Unlike the $(^{H}L)Fe_3(PMe_2R)_3$ analogues, which feature close Fe−Fe contacts (2.299(2)Å),[1a] complex **1** shows much larger ion separation and a greater deviation from an equilateral triangle (Mn1−Mn2 2.8347(6), Mn1−Mn3 2.8291(8), Mn2−Mn3 2.7852(7) Å). Complex **1** more closely resembles the trimagnesium complex $(^{H}L)Mg_3(thf)_3$, which features an average Mg···Mg separation of 2.847(1) Å and more suggestive of the metal ions residing at a distance reflective of simple ionic radii contact as opposed to involvement of metal−metal bonding.[1a] The solution magnetic moment obtained for ^{1}H NMR silent **1** is 5.73(12) μ_B, well below the value expected for three magnetically isolated high-spin Mn^{II} ions (μ_{eff} = 10.25 μ_B). The low moment suggests the presence of

Received: July 16, 2011
Published: September 26, 2011

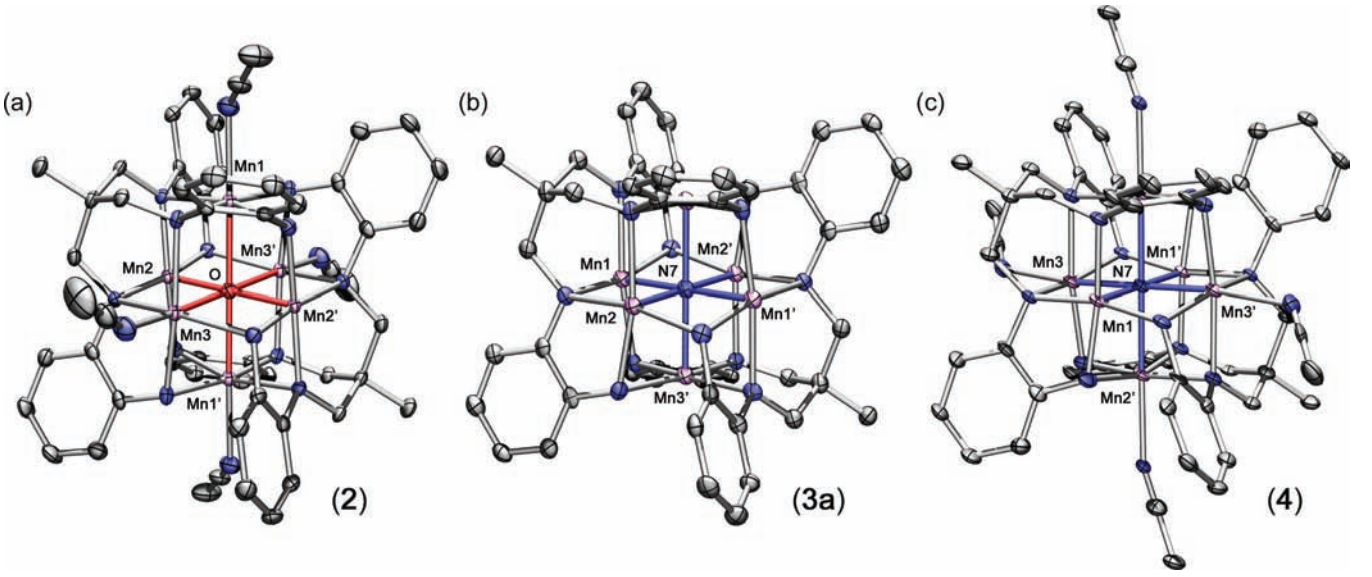

Figure 1. Solid-state structures for (a) $(^{H}L)_2Mn_6(\mu^6\text{-}O)(NCMe)_4$ (**2**), (b) $[(^{H}L)_2Mn_6(\mu^6\text{-}N)](N^nBu_4)_2$ (**3a**), and (c) $(^{H}L)_2Mn_6(\mu^6\text{-}N)(NCMe)_4$ (**4**) with the thermal ellipsoids set at the 50% probability level (hydrogen atoms, solvent molecules, and Bu_4N cations in **3** omitted for clarity; Mn orchid, C black, H white, N blue, O red). Bond lengths (Å) for **2**: Mn1−Mn2, 3.0591(6); Mn1−Mn2′, 3.1394(6); Mn1−Mn3, 3.1143(6); Mn2−Mn3, 3.0442(6); Mn2−Mn3′, 3.0955(6); for **3a**: Mn1−Mn2, 3.0726(8); Mn1−Mn2′, 3.0192(8); Mn1−Mn3, 3.0058(8); Mn1−Mn3′, 3.0694(7); Mn2−Mn3, 3.0120(9); Mn2−Mn3′, 3.0899(8); Mn1−N7, 2.1443(6); Mn2−N7, 2.1634(6); Mn3−N7, 2.1517(5); for **4**: Mn1−Mn2, 3.057(2); Mn1−Mn2′, 3.137(2); Mn1−Mn3, 3.043(2); Mn1−Mn3′, 3.099(2); Mn2−Mn3, 3.116(2).

antiferromagnetic superexchange interactions between Mn^{II} ions through the bridging anilide ligands, similar to the behavior observed in related polynuclear MN^{II} species.[5,6] EPR spectra collected for **1** at 3, 77, and 300 K exhibit an intense isotropic signal with $g = 2.016$, consistent with the presence of an antiferromagnetically coupled system comprised of $S = {}^5/_2$ Mn^{II} ions (see Figures S4, S5, SI).

With **1** in hand, we canvassed its reactivity with both O- and N-atom transfer reagents (Scheme 1). Reaction of **1** with 0.6 equivalents of pyridine N-oxide (or PhIO) results in an immediate color change from orange-red to dark brown. The oxidized product could be crystallized from slow diffusion of diethyl ether into concentrated acetonitrile (NCMe) solutions of the product at room temperature to yield $(^{H}L)_2Mn_6(\mu^6\text{-}O)(NCMe)_4$ (**2**) which we formulate as $Mn^{II}_4\,Mn^{III}_2$, the molecular structure of which is shown in Figure 1a. Use of (4-trifluoromethyl)pyridine *N*-oxide[7] allowed us to confirm consumption of the *N*-oxide via in situ ^{19}F NMR and integration against an internal standard ($C_6H_5CF_3$), suggesting the reaction is quantitative for the O-atom delivery despite the isolated yield of 82% (93% isolated yield using C_5H_5N-O).

Reaction of **1** with one equivalent of tetrabutylammonium azide in tetrahydrofuran at −35 °C results in consumption of 0.5 equivalents of azide, although a color change from **1** does not accompany the reaction as observed in the synthesis of **2**. Cooling solutions of the reaction product in a mixture of hexane and benzene affords crystals of the solvent-free nitride $[(^{H}L)_2Mn_6(\mu^6\text{-}N)](NBu_4)_2$ (**3a**) (93%, Figure 1b), whereas crystallization in the presence of acetonitrile produces the solvated complex, $[(^{H}L)_2Mn_6(\mu^6\text{-}N)(NCMe)_2](NBu_4)_2$ (**3b**, see Figure S12, SI). The presence of two NBu_4 cations indicates the net oxidation to the Mn_6 core is by a single electron ($Mn^{II}_5\,Mn^{III}$). Treatment of **3a** with one molar equivalent of iodine in NCMe rapidly oxidizes the cluster to afford the dark-brown, neutral nitride $(^{H}L)_2Mn_6(\mu^6\text{-}N)(NCMe)_4$ (**4**) with generation of 2 equivalents of $Bu_4N^+I^-$, giving a formulation of $Mn^{II}_3\,Mn^{III}_3$ for **4**. Complex **4** is nearly isostructural with its oxo analogue **2** (Figure 1c). Although crystalline yields for this do not exceed 30%, combustion analysis for the bulk material analyzed was identical to that obtained for single-crystal samples that were crushed and dried in vacuum (to remove solvent from the crystal lattice). While several examples of complexes bearing the $[Mn_6(\mu^6\text{-}O)]$ motif have been previously reported,[8,9] the molecular nitrides **3** and **4** are rather unusual with only one example featuring the $[Mn_6(\mu^6\text{-}N)]$ unit reported in a solid-state structure.[10]

Table 1. Selected Bond Distances (Å)

complex		Mn−X	$Mn-N_H$	$Mn-N_{base}$
2	Mn1	2.2694(4)	2.226(2)	2.245(2)
	Mn2	2.1111(4)	1.997(2)	2.041(2)
	Mn3	2.2289(5)	2.216(2)	2.246(2)
3b	Mn1	2.1178(4)	2.197(2)	2.204(2)
	Mn2	2.1333(4)	2.192(2)	2.226(2)
	Mn3	2.2836(4)	2.217(2)	2.267(3)
4	Mn1	2.111(1)	1.991(6)	2.038(6)
	Mn2	2.267(1)	2.227(6)	2.236(6)
	Mn3	2.230(2)	2.218(6)	2.248(6)

Each of the clusters **2**-**4** consist of an edge-bridged octahedral arrangement of Mn ions, with a μ^6-oxo or nitride ligand situated at the center of the Mn_6 core. This structure is similar to those observed for octahedral $[^{H}L_2Fe_6]$ clusters templated by the $[^{H}L]^{6-}$ ligand, which do not feature interstitial atoms.[1c,d] For the neutral complexes **2** and **4**, two distinct coordination environments are apparent for the Mn ions. First, two trans-disposed Mn sites reside in a square pyramidal coordination environment, with nitrogen atoms of the amide ligands comprising the basal plane and the interstitial bridging atom positioned in the apical site (see Table 1 for selected bond lengths). The remaining four Mn sites each bind a molecule of acetonitrile,

dx.doi.org/10.1021/ja2066384 |*J. Am. Chem. Soc.* 2011, 133, 16750–16753

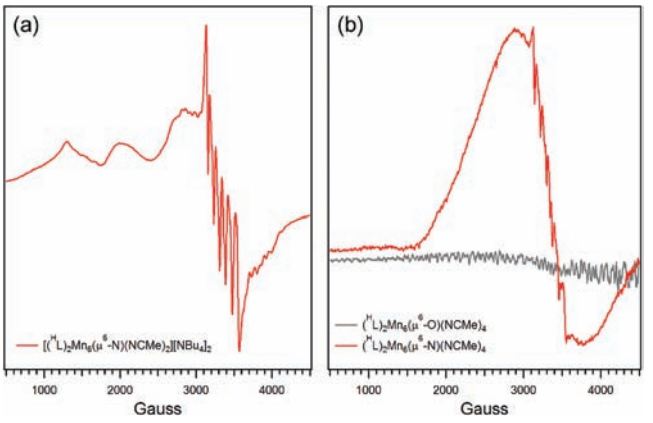

Figure 2. X-band EPR (9.337 GHz) for (a) **3b** (3 K, toluene glass) and spectral overlay for **2** and **4** (77 K, toluene glass).

which completes the octahedral coordination sphere. These sites show elongation of the Mn−X distances and expanded Mn−N_{H_L} interactions, reflective of the different electronic configurations for the square pyramidal Mn^{II} sites $(d_{xy})^1(d_{xz},d_{yz})^2(d_{z^2})^1(d_{x^2-y^2})^1$ and the octahedral Mn^{III} sites $(d_{xy})^1(d_{xz},d_{yz})^2(d_{z^2})^1(d_{x^2-y^2})^0$. Bond valence summation corroborates this assignment with the square pyramidal sites consistent with Mn^{III}, whereas the octahedral sites are consistent with a Mn^{II} formulation.[11]

Unlike the neutral complexes **2** and **4**, there is no obvious structural asymmetry to **3a**. The average Mn−Mn separation is 3.0497(9) Å, comparable to the average distances observed in **2**. The bond metrics from Mn to both amide residues are consistent throughout the core (Mn−N_{base} 2.218(3), Mn−N_H 2.182(3) Å), and are similar to the divalent sites observed in **2**. The Mn−nitride distances show little variance (Mn1−N7 2.1443(6), Mn2−N7 2.1634(6), Mn3−N7 2.1517(5) Å) indicating an equal interaction with the central nitride throughout the Mn_6 core. Indeed, bond valence summation suggests the Mn ions in **3a**, as well as **3b** (see Table 1), more closely resemble divalent manganese than trivalent manganese, suggesting the Mn^{III} site is averaged over all positions in **3a** and within the four solvent-free sites in **3b**.

The solution magnetic moments for the series of compounds: 8.9(3) μ_B for **2**, 8.2(1) for **3b**, and 6.2(1) for **4** are all indicative of antiferromagnetic superexchange coupling between Mn ions through the bridging oxo/nitride and amide ligands. A strong isotropic signal (g = 2.17) is observed by EPR for toluene glasses of **3b** over the temperature range 77−300 K, while cooling to 3 K reveals hyperfine coupling to the Mn ions (I = 5/2) and possibly N (see Figures 2 and S7−S8, SI). The oxidized nitride **4** also exhibits a strong EPR signal with some hyperfine to Mn apparent, consistent with the 27 valence electron formulation, whereas the analogous oxo **2** (28 valence electrons) is EPR silent (Figure 2b).

Given the close structural parameters between the neutral oxo **2** and nitride **4** and the difficulty distinguishing light atom substituents from X-ray analysis,[3c] we sought to identify unequivocally the light interstitial atom via chemical assay. Mass spectral analysis on complexes **2**−**4** proved problematic due to the sensitivity of the $(^{H}L)Mn_3$ units which easily hydrolyze. Thus, we wanted to convert the light atom component into a species we could identify. Protonolysis of the complexes (camphorsulfonic acid, 25 equiv) followed by treatment with benzyl bromide (10 equiv) and base (K_2CO_3, 50 equiv) resulted in alkylation of the central light atom which could be identified by ESI MS. Alkylation of the nitride gave two dominant ions for Bn_3NH^+ ($^m/_z$ 288.1741) and $Bn_2NH_2^+$ ($^m/_z$ 198.1275) that match the predicted isotope pattern and an authentic sample made from the same reaction conditions using the camphorsulfonic acid ammonium salt as a N source (see Figure S10, SI), whereas subjecting **2** to a similar treatment did not reveal those ion peaks. Furthermore, alkylation of 50% isotopically enriched ^{15}N **3b** (synthesized using the isotopically enriched azide $[Na]^{15}NNN$) showed the parent ions for both ^{14}N and ^{15}N isotopologues of Bn_3NH^+ ($^m/_z$ 288.1741; 289.1741) and $Bn_2NH_2^+$ ($^m/_z$ 198.1275; 199.1275).

These results demonstrate the ability to extend our synthetic protocols for the preparation of triiron complexes to prepare an analogous trimanganese complex. Moreover, this complex exhibits similar oxidative, atom-transfer reactivity to the related triiron complexes. The trinuclear manganese complex readily reacts with both O- and N-atom delivery agents to afford $Mn_6(\mu^6\text{-E})$ (E = O, N) clusters, respectively, highlighting the efficacy of using well-defined trinuclear complexes to assemble polynuclear species of higher nuclearity. The clusters likely form via atom transfer to a trimanganese core with subsequent reaction with a second trinuclear complex to yield the hexanuclear products. Work is currently underway to understand the electronic structure of these complexes and canvass the scope of reactivity of the oxidized materials.

■ ASSOCIATED CONTENT

Supporting Information. Experimental procedures and spectral data for **1**−**4**; selected crystallographic data and bond lengths for **1**−**4**; CIF file for **1**, **2**, **3**, **3b**, and **4**; EPR spectra for **1**−**4**. This material is available free of charge via the Internet at http://pubs.acs.org.

■ AUTHOR INFORMATION

Corresponding Author
betley@chemistry.harvard.edu

■ ACKNOWLEDGMENT

We thank Harvard University for financial support and the NIH for an NIH Ruth L. Kirschstein NRSA fellowship for A.R.F. We also thank Prof. Alan Saghatelian and Nawaporn Vinayavekhin for assistance in obtaining the MS data.

■ REFERENCES

(1) (a) Zhao, Q.; Betley, T. A. *Angew. Chem., Int. Ed.* **2011**, *50*, 709–712. (b) Powers, T. M.; Fout, A. R.; Zheng, S.-L.; Betley, T. A. *J. Am. Chem. Soc.* **2011**, *133*, 3336. (c) Zhao, Q.; Harris, T. D.; Betley, T. A. *J. Am. Chem. Soc.* **2011**, *133*, 8293. (d) Harris, T. D.; Zhao, Q.; Hernández Sánchez, R.; Betley, T. A. *Chem. Commun.* **2011**, *47*, 6344. (e) Harris, T. D.; Betley, T. A. *J. Am. Chem. Soc.* **2011**, *133*, 13852.

(2) (a) Adams, R. D. *J. Organomet. Chem.* **2000**, *600*, 1. (b) Suzuki, H. *Eur. J. Inorg. Chem.* **2002**, 1009. (c) Dyson, P. J. *Coord. Chem. Rev.* **2004**, *248*, 2443. (d) Pap, J. S.; DeBeer George, S.; Berry, J. F. *Angew. Chem., Int. Ed.* **2008**, *47*, 10102. (e) Tsui, E. Y.; Day, M. W.; Agapie, T. *Angew. Chem., Int. Ed.* **2011**, *50*, 1668.

(3) (a) Coucouvanis, D. *Acc. Chem. Res.* **1981**, *14*, 201. (b) Pecoraro, V. L.; Baldwin, M. J.; Gelasco, A. *Chem. Rev.* **1994**, *94*, 807. (c) Einsle, O.; Tezcan, F. A.; Andrade, S.; Schmid, B.; Yoshida, M.; Howard, J. B.; Rees, D. C. *Science* **2002**, *297*, 1696. (d) Venkateswara Rao, P.; Holm, R. H. *Chem. Rev.* **2004**, *104*, 527. (e) Lee, S. C.; Holm, R. H. *Chem. Rev.* **2004**, *104*, 1135. (f) Mukhopadhyay, S.; Mandal, S. K.; Bhaduri, S.; Armstrong,

W. H. *Chem. Rev.* **2004**, *104*, 3981. (g) Mullins, C. S.; Pecararo, V. L. *Coord. Chem. Rev.* **2008**, *252*, 416. (h) Hoffman, B. M.; Dean, D. R.; Seefeldt, L. C. *Acc. Chem. Res.* **2009**, *42*, 609.

(4) Anderson, R. A.; Faegri, K., Jr.; Green, J. C.; Haaland, A.; Lappert, M. F.; Leung, W.-P.; Rypdal, K. *Inorg. Chem.* **1988**, *27*, 1782.

(5) Hatnean, J. A.; Raturi, R.; Lefebvre, J.; Leznoff, D. B.; Lawes, G.; Johnson, S. A. *J. Am. Chem. Soc.* **2006**, *128*, 14992.

(6) Tsui, E. Y.; Kanady, J. S.; Day., M. W.; Agapie, T. *Chem. Commun.* **2011**, *47*, 4189.

(7) Jiang, B.; Xiong, W.; Zhang, X.; Zhang, F. *Org. Process Res. Dev.* **2001**, *5*, 531.

(8) (a) Brown, I. D.; Altermatt, D. *Acta Crystallogr., Sect. B* **1985**, *B41*, 244. (b) Thorp, H. H. *Inorg. Chem.* **1992**, *31*, 1585.

(9) (a) Mondal, K. C.; Drew, M. G. B.; Mukherjee, P. S. *Inorg. Chem.* **2007**, *46*, 5625. (b) Stamatatos, T. C.; Pringouri, K. V.; Abboud, K. A.; Christou, G. *Polyhedron* **2009**, *28*, 1624.

(10) Eddine, M. N.; Bertaut, E. F.; Maunaye, M. *Acta Crystallogr., Sect. B* **1977**, *B33*, 2696.

(11) (a) Cavaluzzo, M.; Chen, Q.; Zubieta, J. *Chem. Commun.* **1993**, 131. (b) Brechin, E. K.; Clegg, W.; Murrie, M.; Parsons, S.; Teat, S. J.; Winpenny, R. E. P. *J. Am. Chem. Soc.* **1998**, *120*, 7365. (c) Koo, B.-K.; Lee, U. *Bull. Korean Chem. Soc.* **2001**, *22*, 103. (d) Bagai, R; Abboud, K. A.; Christou, G. *Inorg. Chem.* **2008**, *47*, 621.